Nanofibrous nerve conduits for repair of 30-mm-long sciatic nerve defects

Esmaeil Biazar[1], Saeed Heidari Keshel[2, 3], Majid Pouya[4], Hadi Rad[4], Melody Omrani Nava[4], Mohammad Azarbakhsh[5], Shirin Hooshmand[5]

1 *Department of Biomaterial Engineering, Tonekabon Branch, Islamic Azad University, Tonekabon, Iran*
2 *Student Research Committee, Proteomics Research Center, Faculty of Paramedical Sciences, Shahid Beheshti University of Medical Sciences, Tehran, Iran*
3 *Department of Tissue Engineering, School of Advanced Technologies in Medicine, Tehran University of Medical Sciences, Tehran, Iran*
4 *Department of Medical Sciences, Tonekabon Branch, Islamic Azad University, Tonekabon, Iran*
5 *Faculty of Medical Sciences, Babol University of Medical Sciences, Babol, Iran*

Research Highlights

(1) This study used a poly(3-hydroxybutyrate-co-3-hydroxyvalerate) nerve conduit, which has been shown to possess satisfactory biocompatibility and biodegradability, to repair a 30-mm-long sciatic nerve defect.

(2) At 4 months after surgery, the diameter of regenerated myelinated nerve fibers on the operated side of rats in the nanofibrous group was similar to that in the autograft group, the regenerated sciatic nerve fibers were continuous, myelinated and grew toward target skeletal muscle.

(3) Results from this study offer a novel solution for repair of long-segment peripheral nerve defects in the clinic.

Abstract

It has been confirmed that nanofibrous poly(3-hydroxybutyrate-co-3-hydroxyvalerate) nerve conduit can promote peripheral nerve regeneration in rats. However, its efficiency in repair of over 30-mm-long sciatic nerve defects needs to be assessed. In this study, we used a nanofibrous poly(3-hydroxybutyrate-co-3-hydroxyvalerate) nerve conduit to bridge a 30-mm-long gap in the rat sciatic nerve. At 4 months after nerve conduit implantation, regenerated nerves were cally observed and histologically assessed. In the nanofibrous graft, the rat sciatic nerve trunk had been reconstructed by restoration of nerve continuity and formation of myelinated nerve fiber. There were Schwann cells and glial cells in the regenerated nerves. Masson's trichrome staining showed that there were no pathological changes in the size and structure of gastrocnemius muscle cells on the operated side of rats. These findings suggest that nanofibrous poly(3-hydroxybutyrate-co-3-hydroxyvalerate) nerve conduit is suitable for repair of long-segment sciatic nerve defects.

Key Words

neural regeneration; peripheral nerve injury; sciatic nerve; artificial conduit; nanofiber; poly(3-hydroxybutyrate-co-3-hydroxyvalerate); macroscopic observation; histology; grants-supported paper; neuroregeneration

INTRODUCTION

Peripheral nerves form an extensive network that links the central nervous system to all other parts of the body[1-3]. Peripheral nerve injury can interrupt communication between the brain and the muscles controlled by a nerve, affecting a person's ability to move certain muscles or normal sensations[4]. Damaged peripheral nerves have been reconstructed by different methods, including allograft techniques, cell therapy (Schwann cells, stem cells, fibroblasts and olfactory cells), drug therapy, use of biological tubes and the designed scaffolds with synthetic and natural materials or absorbable and non-absorbable synthetic and natural polymers with unique features[5-7].

Autografts or allografts are commonly used in surgery. However, autografts have limitations for example body injury, repeated surgeries and disproportion of grafted nerve tissue in size and structure[8-9]. Similar problems have been encountered in allografting or xenografting, for example, stimulation of the immune system is required[10-14]. Many studies in which artificial neural tubes are used to repair nerve defects have been performed[15-17]. There is clinical evidence that functional improvement and regeneration of peripheral nerve tissue can be acquired after using silicone tubes to repair 3–5 mm-long peripheral nerve defects[18]. Poly(L-lactic acid) hollow tube is one of scaffolds successfully used for rebuilding sciatic nerve fibers with nerve tissue gaps of 14–18 mm. Biodegradable sutures composed of polyamide fibers show similar results in repair of 7–15 mm sciatic nerve defects, but they are not suitable for longer sciatic nerve gaps[18]. Among these synthetic polymers, poly(3-hydroxy-butyrate-co-3-hydroxyvalerate) (PHBV) microbial polyester has been preferred as it is a biocompatible and biodegradable copolymer. PHBV is a material with suitable properties for cellular growth and adhesion with controllable degradation[19-20]. Nanofibers have improved the performance of biomaterials[21-30]. The purpose of this study is to investigate the feasibility of PHBV conduits in the repair of 30-mm sciatic nerve gap in a rat model using macroscopic observation and histological assessment.

RESULTS

Quantitative analysis of experimental animals

Twenty initially included male Wistar rats were randomly and evenly divided into control, nanofibrous conduit and autograft, polymeric film conduit groups. In the latter groups, nanofibrous conduit, autograft and polymeric film conduit were used to bridge a 30-mm-long sciatic nerve defect, respectively. No additional intervention was given in the control group with the exception of sciatic nerve defect. All 20 rats were included in the final analysis.

Characterization of nanofibrous conduits

The ultrastructure of nanofibrous conduits designed by electro-spinning method at various magnifications is shown in Figure 1. Smooth and homologous nanofibers are clearly shown in Figure 1B. The average diameter obtained for the nanofibers was about 100 nm.

The nanofibrous PHBV nerve conduit showed a porosity of 95.62%, scaffold pore size of 0.45 ± 0.25 μm, contact angle of 105 ± 3.2 degrees and a specific surface area of 138 m^2/g. In addition, the tensile modulus (110 ± 18 MPa) and ultimate tensile strength (5.9 ± 0.5 MPa) of the nanofibrous PHBV nerve conduit were suitable for mechanical stresses. It is clear that the designed polymeric conduits are suitable for axon movement and nerve regeneration.

Viability and attachment of cultured Schwann cells

(3-(4,5-Dimethylthiazol-2-yl)-2,5-diphenyltetrazolium bromide) (MTT) assay showed that the viability of the cultured Schwann cells was 100%, 60% and 90% respectively for the control (TCPS), the nanofibrous PHBV mat and the polymeric film. Cell attachment efficiency to the nanofibrous samples was

high. Figure 2 shows a good cultured cell growth in the vicinity of nanofibrous mat. Figure 3 shows the scanning electron microscopy images of cultured Schwann cells on the polymeric samples. Figures 2, 3 show good cell attachment of Schwann cells on nanofibrous surfaces.
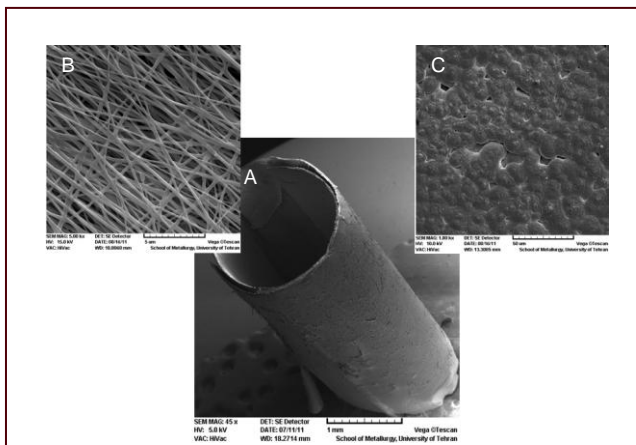

Figure 1 Ultrastructure of nanofibrous nerve conduit as shown by scanning electron microscopy.

(A) Tubular conduit (× 45; scale bar: 1 mm). (B) The nanofibrous structure of designed conduit (× 5 000; scale bar: 5 μm). (C) The structure of polymeric film (× 1 000; scale bar: 50 μm).
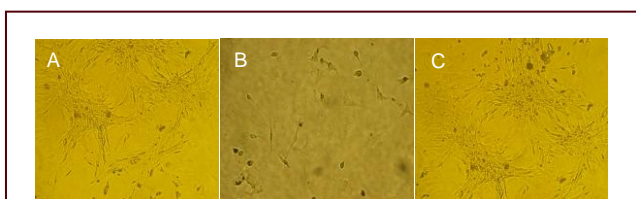

Figure 2 Growth of cultured Schwann cells as shown by optical microscope (× 200).

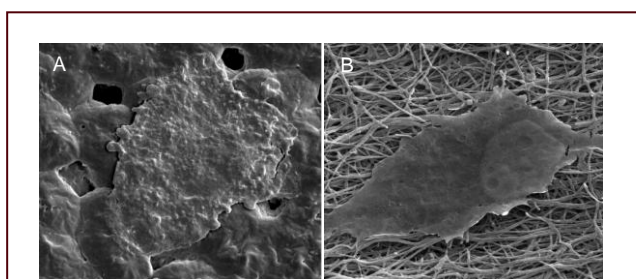Cultured Schwann cells grew on the control sample (A), the polymeric film (B), and the nanofibrous mat (C).

Figure 3 Ultrastructure of Schwann cells that attach and spread on the polymeric surfaces as shown by scanning electron microscopy (× 2 000).

(A) Polymeric film; (B) nanofibrous mat.

Macroscopic results of regenerated nerve

Figure 4 shows the regenerated sciatic nerve at 4 months after surgery. Reconstructed nerves were not observed in the control group, but sciatic nerve regene-

ration and neural cord formation were observed in the autograft, polymeric film conduit and nanofibrous conduit groups.
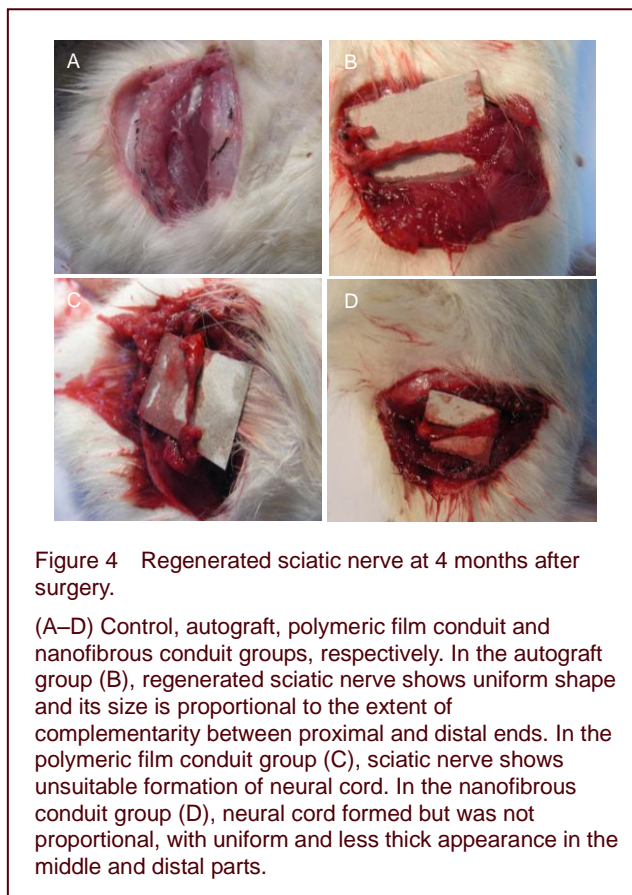

Figure 4 Regenerated sciatic nerve at 4 months after surgery.

(A–D) Control, autograft, polymeric film conduit and nanofibrous conduit groups, respectively. In the autograft group (B), regenerated sciatic nerve shows uniform shape and its size is proportional to the extent of complementarity between proximal and distal ends. In the polymeric film conduit group (C), sciatic nerve shows unsuitable formation of neural cord. In the nanofibrous conduit group (D), neural cord formed but was not proportional, with uniform and less thick appearance in the middle and distal parts.

Histological and morphological characterizations of sciatic nerve

Microscopic images of the middle section of stained sciatic nerve with toluidine blue are shown in Figure 5. At 4 months after surgery, suitable regenerated nerve fibers with myelin sheet were observed in the autograft group, and myelinated nerve fibers formed in the nanofibrous conduit group but were not observed in the polymeric film conduit group. Figure 6 shows the thickness of myelinated nerve fibers after 4 months. The myelin sheath thickness in the polymeric film conduit, nanofibrous conduit and autograft groups was 0.26 ± 0.03, 0.35 ± 0.02 and 0.85 ± 0.04 μm, respectively. The average myelin sheath thickness in the nanofibrous conduit group was less than in the autograft group ($P < 0.05$).

Polymeric film conduits and nanofibrous conduits can increase the expression of S-100 and glial fibrillary acidic protein (GFAP), cellular markers of Schwann cells and glial cells in injured nerve tissue. Figure 6 shows the expression of S-100 and GFAP in the sciatic nerve samples harvested from the autograft, polymeric film conduit and nanofibrous conduit groups.
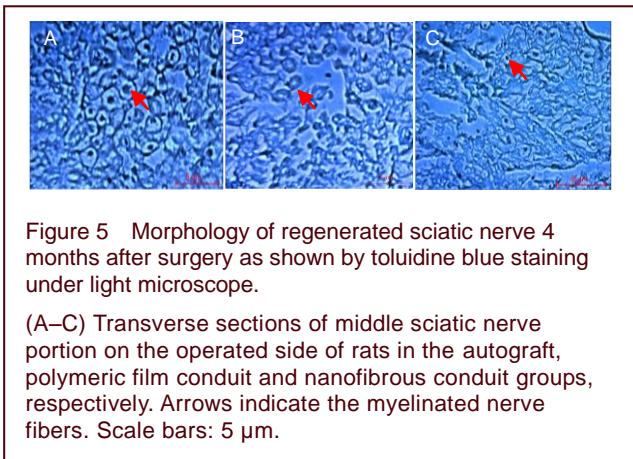
Figure 5   Morphology of regenerated sciatic nerve 4 months after surgery as shown by toluidine blue staining under light microscope.

(A–C) Transverse sections of middle sciatic nerve portion on the operated side of rats in the autograft, polymeric film conduit and nanofibrous conduit groups, respectively. Arrows indicate the myelinated nerve fibers. Scale bars: 5 μm.
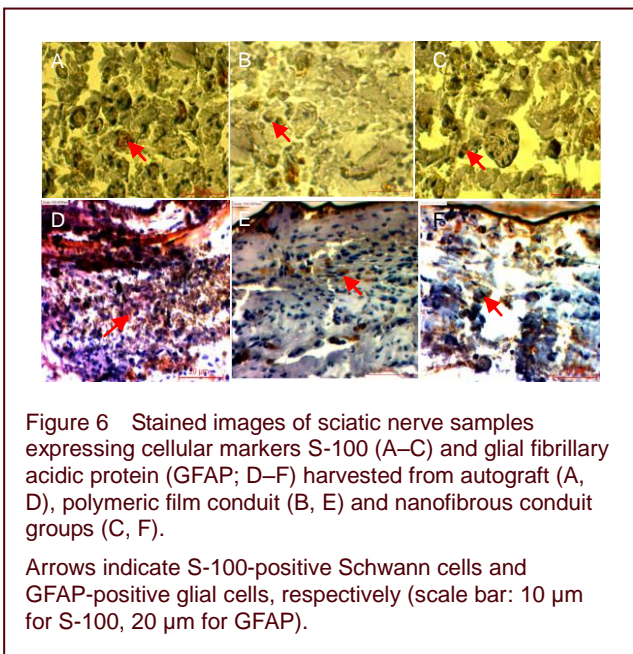

Figure 6   Stained images of sciatic nerve samples expressing cellular markers S-100 (A–C) and glial fibrillary acidic protein (GFAP; D–F) harvested from autograft (A, D), polymeric film conduit (B, E) and nanofibrous conduit groups (C, F).

Arrows indicate S-100-positive Schwann cells and GFAP-positive glial cells, respectively (scale bar: 10 μm for S-100, 20 μm for GFAP).

some drawbacks.

Figure 7   Light micrographs of the sectioned gastrocnemius muscle following Masson's trichrome staining 4 months after surgery in the control (A), autograft (B), polymeric film conduit (C) and nanofibrous conduit groups (D).

Arrowheads indicate atrophic muscle cells and arrows pointed at the hyperplastic adipocytes.
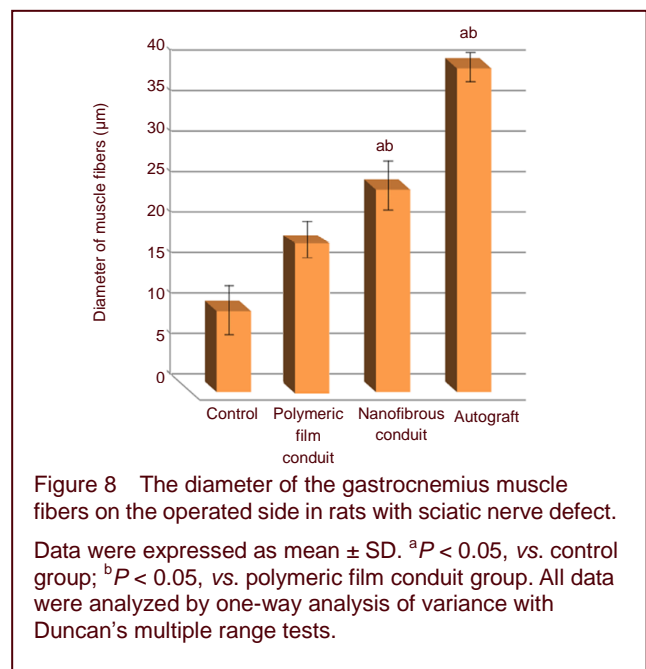
Figure 8   The diameter of the gastrocnemius muscle fibers on the operated side in rats with sciatic nerve defect.

Data were expressed as mean ± SD. $^a P < 0.05$, *vs.* control group; $^b P < 0.05$, *vs.* polymeric film conduit group. All data were analyzed by one-way analysis of variance with Duncan's multiple range tests.

Masson's trichrome staining results of the gastrocnemius muscles of rats from the control, autograft, polymeric film conduit and nanofibrous conduit groups at 4 months after surgery are shown in Figure 7. The muscle cells exhibited homogeneous and regular structure in the autograft samples. The fiber diameter in the sciatic nerve samples from the polymeric film conduit, nanofibrous conduit and autograft groups was 17, 25 and 40 μm, respectively. The diameter distribution of myelinated nerve fibers at the middle sciatic nerve portion of the rat operated side was similar between the nanofibrous conduit group and the autograft group (Figure 8).

DISCUSSION

For peripheral nerve repair, a lot of scientific effort has been devoted to developing artificial nerve grafts to replace traditional autograft techniques, which exhibit

Although artificial nerve grafts made of non-resorbable materials (*e.g.*, conduits made of silicone or polyethylene) can promote functional recovery, long-term complications often mean that a second surgical procedure is necessary to remove the conduits. These may actually become detrimental by virtue of toxicity or tendency to constrict the nerve[31]. A nerve graft made of bioresorbable materials is thus a promising alternative for promoting successful nerve regeneration. From this perspective,

the PHBV tube is a candidate that might replace the nerve graft, at least for repair of long segment nerve defects[32-34]. The conduit is very easy to be handled; it can be easily placed and sutured on the nerve, thus eliminating the need of a very accurate nerve suture technique[34]. The electrospinning technique is widely recognized as a straightforward way to fabricate nanoscale fibrous structures. Since this technique can produce nano- or submicron fibrous scaffolds which mimic the structure of natural extracellular matrix, it has elicited extensive research interest[35].

In this study, the nanofibrous conduit showed suitable physical, mechanical and structural properties as the nerve autograft. At 4 months after surgery, the diameter distribution of myelinated nerve fibres at the middle sciatic nerve portion on the operated side of rats in the nanofibrous conduit group was similar to that in the autograft group, the regenerated sciatic nerve fibers were continuous, myelinated and grew toward target skeletal muscle. However, several studies have shown that the diameter of myelinated nerve fibers was usually small during a short period of time[36-39]. It is known that denervation of a target muscle occurs as a consequence of damage to motor nerves, followed by alterations in various aspects including gene expression, protein metabolism, enzyme activity, cell ultrastructure and neuromuscular junction. This induces a shift of protein metabolism from protein synthesis toward protein degradation, an increase in muscle fiber size, and muscular atrophy accompanied by hyperplasia of connective tissues. If the muscle is reinnervated, its function is restored and atrophy is stopped[40-42]. There were morphological differences between the nanofibrous conduit group and the control group. The nuclei of control group were under the sarcolemma, with no remarkable increase in number, and they showed clear cross striations on longitudinal sections, but the grafted samples with the nanofibrous conduit show a semi-regular shape compared to the autograft sample. The muscles on the operated side were red and lustrous in color, and quite soft in texture in both the nanofibrous conduit and autograft groups. However, they were pale in color, hard and tenacious in texture with the severely atrophic muscle belly in the control and polymeric film conduit groups. In the control and non-fibrous conduit groups, gastrocnemius cells on the operated side exhibited typical atrophy and degeneration resulting from denervation with hyperplasia; the cross-sectional area of muscle cells was much smaller, being a half of that in the nanofibrous conduit group. Taken together, in this study, tubular, biodegradable, polymeric nerve conduits were designed for use in res-

toration of the function of injured nerve tissues. The polymeric film nerve conduits and nanofibrous PHBV nerve conduits were used to bridge 30-mm-long sciatic nerve gaps. The nanofibrous conduits showed suitable physical and structural properties as the nerve autograft. At 4 months after surgery, the sciatic nerve truck had been reconstructed by restoration of nerve continuity, formation of myelinated nerve fibers, and reinnervation of target skeletal muscle. Accordingly, this study proves the feasibility of the nanofibrous nerve graft in promoting nerve regeneration, raises new possibilities of seeking alternatives to autografts for nerve repair, and establishes an experimental basis for constructing tissue engineered nerve grafts favorable to an implantation into the peripheral nerve with a larger defect. Furthermore, this study offers a novel solution for repair of long-segment peripheral nerve defects in the clinic.

MATERIALS AND METHODS

Design
A controlled, observational study.

Time and setting
This study was performed at Department of Biomedical Engineering, Tonekabon Branch, Islamic Azad University, Tonekabon, Iran between January 2011 and September 2012.

Materials
Twenty male Wistar rats, aged 4–8 weeks and weighing 180–220 g, were included in the study. The experimental protocol was approved by the Institutional Animal Care and Use Committee of Shahid Beheshti University of Medical Sciences (Iran). All experimental procedures were performed in strict accordance with the guidelines established for animal care by the Proteomics Research Center, Beheshti University of Medical Sciences, Iran.

Methods
Design of nanofibrous scaffolds
PHBV with the molecular weight of 680 000 was purchased from Sigma Chemical Co., Ltd., China. 2,2,2-trifluoroethanol (TFE), which was used to prepare PHBV solution, was also purchased from Sigma and used as received, without further purification. Electrospinning apparatus used in this study was prepared by Fanavaran Nano-Meghyas Company (Iran). The prepared PHBV solution (2% w/v) was pumped into a glass syringe controlled by syringe pump. A positive high voltage source through a wire was applied at the tip of a

syringe needle. In this situation, a strong electric field (20 kV) was generated between PHBV solution and a collector. When the electric field reached a critical value with increasing voltage, mutual charge repulsion overcame the surface tension of the polymer solution and an electrically charged jet was ejected from the tip of a conical shape as the Taylor cone. Ultrafine fibers are formed by narrowing the ejected jet fluid as it undergoes increasing surface charge density due to the evaporation of the solvent. An electrospun PHBV mat was carefully detached from the collector and dried in a vacuum for 2 days at room temperature to remove solvent molecules completely. The nanofibrous mat was designed with certain parameters namely: syringe size: 17 mm; collector speed: 1 000 r/min; injection speed: 2 mL/min; syringe tip distance to collector: 75 mm; voltage: 20 kV; temperature: 30°C; time: 7 hours.

Design of polymeric film

A PHBV solvent cast film was used as control substrate. To prepare the film, 10 mL PHBV/TFE solution was spread on a glass plate and the solvent was evaporated at room temperature. The concentrated PHBV solution was then irradiated by an infrared lamp to evaporate the residual solvent.

Characterization of nanofibrous conduits

The surface characteristics of electrospun mats were investigated by a scanning electron microscope (Cambridge Stereo-scan, S-360, Wetzlar, Germany). The mats were first gold-sputtered for 2 hours (Ion Sputter, JFC-1100, JOEL, Japan) to provide surface conduction before scanning. The static contact angles were investigated by a contact angle measuring apparatus (Krüss G10; Krüss, Matthews, NC, Germany) for the sessile drop method[32]. For mechanical investigations, the mats were subjected to stress-strain analysis using a universal testing machine under an extension rate of 5 mm/min and 100 N load cells[32]. The specific surface area of nanofibrous mats were determined by the surface area and pore size analyzer[31].

Schwann cell culture

Schwann cells were obtained from sciatic nerves of adult Wistar rats according to an earlier described method[43]. In brief, sciatic nerve segments were washed in DMEM/F12 twice, re-suspended in 0.3% collagenase type II solution (100 µL per segment) and incubated for 30 minutes at 37°C. After incubation, the enzymatic solution was carefully removed, and an equal volume of 0.25% trypsin-EDTA was added. Then the sciatic nerve segments were incubated for another 5 minutes at 37°C

and then mechanically dissociated until they formed a homogeneous suspension. Schwann cell basal medium was added to the suspension at a ratio of 4:1 in order to terminate the activity of the trypsin. The mixture was centrifuged at 800–1 000 r/min for 5 minutes. After supernatant removal, the cells were re-suspended in Schwann cell basal medium. Schwann cells were proliferated in the flask and washed with PBS for subculture. Then trypsin enzyme/EDTA was added to the flask (37°C) and incubated for 90 seconds. Fetal bovine serum (FBS)/DMEM culture media was added to the flask and the cells were gently pipetted. Subsequently, the cell suspension was transferred to a tube (15 mL) (BD Bioscience, San Jose, CA, USA) and centrifuged ($400 \times g$) (Eppendorf Int. 5702 model, Germany) for 5 minutes. After removal of solution, the precipitates were transferred to a new flask (75 cm) for culture again.

Cell cultures (1 cm × 1 cm) from the Petri dish (Control) and the main samples were individually placed in the Petri dish wells using a sterilized pincer. Cells were seeded into a 24-well culture plate at a density of 2×10^5 cells/well and then removed by a pipette and poured onto the control, the polymeric film and nanofibrous mat. Afterwards, all samples were placed in a binder incubator at 37°C for 48 hours and observed under an inverted microscope (Wolf Laboratories, UK). Cell growth and viability were analyzed with the MTT (Sigma-Aldrich) assay. The yellow dye MTT was reduced to a blue formazan product by respiratory enzymes which are active only in viable cells, indicating cell proliferation. Briefly, 5 000 Schwann cells were seeded on PHBV scaffolds. For analysis, 20 µL of MTT substrate (Sigma-Aldrich; 2.5 mg/mL stock solution in PBS) was added to each well, and the plates were placed in the standard tissue incubation conditions for an additional 4 hours. After removal of medium, cells were solubilized in 100 µL of dimethyl sulfoxide, and colorimetric analysis was performed. For microscopic observation, the cultured scaffolds with Schwann cells were washed by PBS and then fixed by glutheraldehyde (2.5 %) at 4°C for 2 hours. The samples were dehydrated by alcohols and treated with tetraoxide osmium vapors at 4°C for 2 hours. Then they were coated with gold and observed under a scanning electron microscope (Cambridge Stereo-scan, S-360, Wetzlar, Germany).

Preparation of three-dimensional nerve conduits

The polymeric sheets (Figure 9A) (33 mm in length and 5 mm in width) were rolled around the cylindrical rod to form a three-dimensional tubular structure and maintained in this form using a thermal agent[32, 44] (Figure 9B, C).
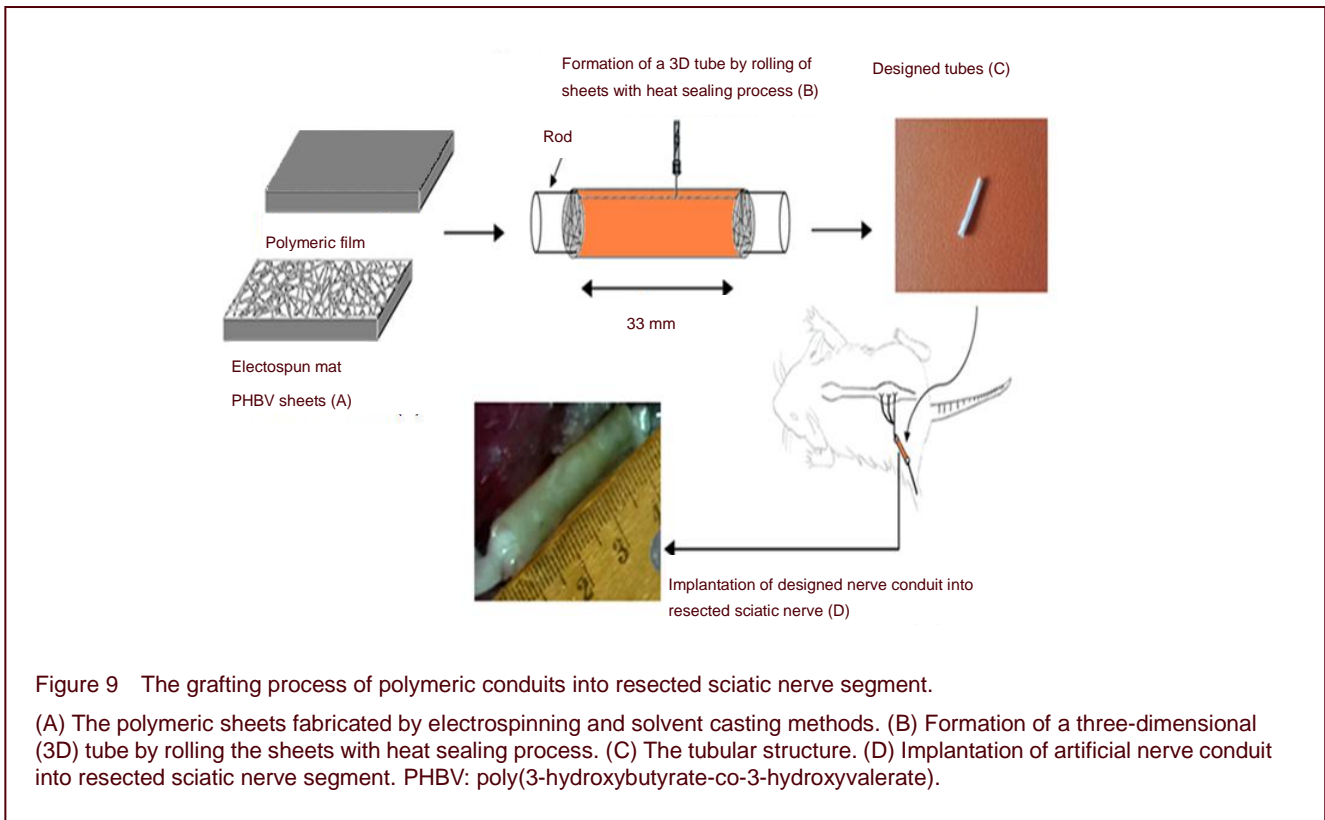
Figure 9 The grafting process of polymeric conduits into resected sciatic nerve segment.

(A) The polymeric sheets fabricated by electrospinning and solvent casting methods. (B) Formation of a three-dimensional (3D) tube by rolling the sheets with heat sealing process. (C) The tubular structure. (D) Implantation of artificial nerve conduit into resected sciatic nerve segment. PHBV: poly(3-hydroxybutyrate-co-3-hydroxyvalerate).

Establishment of sciatic nerve defect rat models and implantation of artificial nerve grafts

A long segment of sciatic nerve was resected, leaving a 30 mm gap caused by retraction of nerve endings. In the autograft group, a 30 mm segment of sciatic nerve was excised, reversed and sutured back in place. In the nanofibrous and polymeric tubes of 33 mm in length were used so that the two nerve ends could be slided for 1.5 mm into the tube and anchored with two epi-perineural sutures. A 30 mm gap was thus maintained between the nerve stumps inside the tube. After surgery, the animals were placed in separate cages. All animals had free access to standard rat food and water.

Macroscopic analysis

At 4 months after surgery, the rats were sacrificed and the regenerated nerves in the control, autograft and xenograft groups were resected for macroscopic analysis.

Histological and morphological analysis

For histological analysis, rat middle sciatic nerve cords were removed and fixed in 10% formalin at 4°C for 5 days, dehydrated and then paraffin-embedded. Serial 2 μm paraffin sections were cut with a Senior Precision Rotary Microtome (Model-RMT-30, India), stained with toluidine blue (Sigma, St. Louis, MO, USA) according to routine histology protocol and examined by an optical microscope (Carl Zeiss, Oberkochen, Germany). Myelin thickness was calculated based on Image J software (version 1.41; National Institutes of Health, Rockville, MD, USA). The gastrocnemius muscles were harvested from the operated limbs of rats in all groups, fixed in 5% glutaraldehyde aqueous solution, and then cut into 10 μm thick sections. Then the sections were stained by Masson's trichrome staining and observed under the optical microscope (Nikon, Japan). The average diameter of the muscle fibers was analyzed using the image analysis system (Image J software; version 1.41; National Institutes of Health, Rockville, MD, USA).

For immunohistochemical analysis, sections were treated with heated antigen retrieval solution and then immersed in 3% H_2O_2 solution to block the endogenous peroxidase. After being incubated with normal goat serum for 30 minutes to block the nonspecific antibody binding sites, the sections were incubated with primary antibodies including rabbit anti-rat GFAP as cellular marker of glial cells (CK; 1:100; Chemicon, Temecula, CA, USA) and rabbit anti-rat S100 as cellular marker of Schwann cells (1:200; Chemicon) at 4°C overnight. After PBS washes, cells were incubated with either horseradish peroxidase-conjugated goat anti-mouse or anti-rabbit secondary antibody (DAKO, Glostrup, Denmark) and visualized with 3,3'-diaminobenzidine tetrahydrochloride (DAKO). Then the sections were stained with hematoxylin and

observed by a light microscope. Blank control sections were treated in the way described earlier, with the exception of use of PBS instead of primary antibody.

Statistical analysis

Data were analyzed using SPSS 16.0 (SPSS, Chicago, IL, USA) and were expressed as mean ± SD and analyzed by one-way analysis of variance with Duncan's multiple range test. A level of $P < 0.05$ was considered statistically significant.

REFERENCES

[1] Hughes RA. Peripheral neuropathy. BMJ. 2002; 324(7335):466-469.

[2] Burnett MG, Zager EL. Pathophysiology of peripheral nerve injury: a brief review. Neurosurg Focus. 2004;16:E1.

[3] Yin Q, Kemp GJ, Frostick SP. Neurotrophins, neurones and peripheral nerve regeneration. J Hand Surg Br. 1998; 23:433-437.

[4] Biazar E, Khorasani MT, Montazeri N, et al. Types of neural guides and using nanotechnology for peripheral nerve reconstruction. Int J Nanomedicine. 2010;5:839-852.

[5] Ghaemmaghami F, Behnamfar F, Saberi H. Immediate grafting of transected obturator nerve during radical hysterectomy. Int J Surg. 2009;7:168-169.

[6] Firouzi M, Moshayedi P, Saberi H, et al. Transplantation of Schwann cells to subarachnoid space induces repair in contused rat spinal cord. Neurosci Lett. 2006;402:66-70.

[7] Ducker TB, Hayes GJ. Peripheral nerve grafts: experimental studies in the dog and chimpanzee to define homograft limitations. J Neurosurg. 1970;32:236-243.

[8] Evans GR. Tissue engineering strategies for nervous system repair. Prog Brain Res. 2000;128:349-363.

[9] Heath CA, Rutkowski GE. The development of bioartificial nerve grafts for peripheral nerve regeneration. Trends Biotechnol. 1998;16:163-168.

[10] Brunelli GA, Battiston B, Vigasio A, et al. Bridging nerve defects with combined skeletal muscle and vein conduits. Microsurgery. 1993;14:247-251.

[11] Tong XJ, Hirai K, Shimada H, et al. Sciatic nerve regeneration navigated by laminin-fibronectin double coated biodegradable collagen grafts in rats. Brain Res. 1994;663:155-162.

[12] Fansa H, Schneider W, Wolf G, et al. Host responses after acellular muscle basal lamina allografting used as a matrix for tissue engineered nerve grafts. Transplantation. 2002;74:381-387.

[13] Barcelos AS, Rodrigues AC, Silva MD, et al. Inside-out vein graft and inside-out artery graft in rat sciatic nerve repair. Microsurgery. 2003;23:66-71.

[14] Godard CW, de Ruiter MD, Spinner RJ, et al. Nerve tubes for peripheral nerve repair. Neurosurg Clin N Am. 2009;1:91-105.

[15] Archibald SJ, Shefner J, Krarup C, et al. Monkey median nerve repaired by nerve graft or collagen nerve guide tube. J Neurosci. 1995;15:4109-4123.

[16] Fields RD, Le Beau JM, Longo FM, et al. Nerve regeneration through artificial tubular implants. Prog Neurobiol. 1989;33:87-134.

[17] Keeley R, Atagi T, Sabelman E, et al. Peripheral nerve regeneration across 14-mm gaps: A comparison of autograft and entubulation repair methods in the rat. J Reconstr Microsurg. 1993;9:349-358.

[18] Lundborg G, Rosen B, Dahlin L, et al. Tubular versus conventional repair of median and ulnar nerves in the human forearm: Early results from a prospective, randomized, clinical study. J Hand Surg. 1997;22:99-106.

[19] Williams SF, Martin DP, Horowitz DM, et al. PHA applications: addressing the price performance issue: I. Tissue engineering. Int J Biol Macromol. 1999;25:111-121.

[20] Liu J, Zhao B, Zhang Y, et al. PHBV and predifferentiated human adipose-derived stem cells for cartilage tissue engineering. J Biomed Mater Res A. 2010;94(2):603-610.

[21] Hromadka M, Collins JB, Reed C, et al. Nanofiber applications for burn care. J Burn Care Res. 2008;29:695-703.

[22] Venugopal J, Low S, Choon AT, et al. Interaction of cells and nanofiber scaffolds in tissue engineering. J Biomed Mater Res B Appl Biomater. 2008;84:34-48.

[23] Majdi A, Biazar E, Heidari S. Fabrication and comparison of electro-spun PHBV nanofiber and normal film and its cellular study. Orient J Chem. 2011;27:523-528.

[24] Biazar E, Zhang Z, Heidari S. Cellular orientation on micro-patterned biocompatible PHBV film. J Paramed Sci. 2010;1:74-77.

[25] Rezaei tavirani M, Biazar E, Ai J, Heidari S, et al. Fabrication of collagen-coated poly (beta-hydroxy butyrate-co-beta-hydroxyvalerate) nanofiber by chemical and physical methods. Orient J Chem. 2011;27:385-395.

[26] Ai J, Heidari S, Ghorbani F, Ejazi F, et al. Fabrication of coated-collagen electrospun PHBV nanofiber film by plasma method and its cellular study. J Nanomater. 2011; 2011:1-8.

[27] Heidari S, Biazar E, Rezaei tavirani M. Reconstructing calvarial bone lesions using PHBV scaffolds and cord blood mesenchymal stem cells in rat. Journal of Kermanshah University of Medical Sciences. 2013;16:600-609.

[28] Heidari S, Biazar E, Rezaei tavirani M, et al. The healing effect of unrestricted somatic stem cells loaded in collagen-modified nanofibrous PHBV scaffold on full-thickness skin defects. Artif Cell Nanomed Biotech. in press.

[29] Biazar E, Heidari S. Rat sciatic nerve regeneration across a 30-mm defect bridged by a nanofibrous PHBV and Schwann cell as artificial nerve graft. Cell Commun Adhes. 2013;20:41-49.

[30] Biazar E, Heidari S. Effects of chitosan cross linked nanofibrous PHBV scaffold combined with mesenchymal stem cells on healing of full-thickness skin defects. J biomed nanotechnol. 2013;9:1471-1482.

[31] Fields RD, Le Beau JM, Longo FM, et al. Nerve regeneration through artificial tubular implants. Prog Neurobiol. 1989;33:87-134.

[32] Yucel D, Kose GT, Hasirci V. Polyester based nerve guidance conduit design. Biomaterials. 2010;31:1596-1603.

[33] Kalbermatten DF, Erba P, Mahay D, et al. Schwann cell strip for peripheral nerve repair. J Hand Surg Eur Vol. 2008;33:587-594.

[34] Xiao XQ, Zhao Y, Chen GQ. The effect of 3-hydroxybutyrate and its derivatives on the growth of glial cells. Biomaterials. 2007;28:3608-3616.

[35] Meng W, Xing ZC, Jung KH. Synthesis of gelatin-containing PHBV nanofiber mats for biomedical application. J Mater Sci Mater Med. 2008;19:2799-2807.

[36] Kiyotani T, Teramachi M, Takimoto Y, et al. Nerve regeneration across a 25-mm defect bridged by a polyglycolic acid-collagen tube: a histological and electrophysiological evaluation of regenerated nerves. Brain Res. 1996;740: 66-74.

[37] Ceballos D, Navarro X, Dubey N, et al. Magnetically aligned collagen gel filling a collagen nerve guide improves peripheral nerve regeneration. Exp Neurol. 1999; 158:290-300.

[38] Fine EG, Decosterd I, Papaloizos M, et al. GDNF and NGF released by synthetic guidance channels support sciatic nerve regeneration across a long defect. Eur J Neurosci. 2002;15:589-601.

[39] Matsumoto K, Ohnishi K, Kiyotani T, et al. Peripheral nerve regeneration across an 80-mm defect bridged by a polyglycolic acid (PGA)-collagen tube filled with laminin-coated collagen fibres: a histological and electrophysiological evaluation of regenerated nerves. Brain Res. 2000;868:315-328.

[40] Bodine SC, Latres E, Baumhueter S, et al. Identification of ubiquitin ligases required for skeletal muscle atrophy. Science. 2001;294:1704-1708.

[41] Bodine-Fowler SC, Allsing S, Botte MJ. Time course of muscle atrophy and recovery following a phenol-induced nerve block. Muscle Nerve. 1996;19:497-504.

[42] Ijkema-Paassen J, Meek MF, Gramsbergen A. Transection of the sciatic nerve and reinnervation in adult rats: muscle and endplate morphology. Equine Vet J Suppl. 2001;33:41-45.

[43] Wei Y, Zheng Z, Wang A, et al. An improved method for isolating Schwann cells from postnatal rat sciatic nerves. Cell Tissue Res. 2009;337:361-369.

[44] Sinis N, Kraus A, Tselis N, et al. Functional recovery after implantation of artificial nerve grafts in the rat – a systematic review. J Brachial Plex Peripher Nerve Inj. 2009;4:19.

(Reviewed by DeCoster MA, Wu M, Zhang N, Wang LS)
(Edited by Li CH, Song LP, Liu WJ, Zhao M)